Journal of The Electrochemical Society, **150** (3) C99-C103 (2003)
0013-4651/2003/150(3)/C99/5/$7.00 © The Electrochemical Society, Inc.

Surface Growth of Ni Thin Films Electrodeposited on Ni(100) Surfaces

M. Saitou,*,z K. Hamaguchi, and W. Oshikawa

Department of Mechanical Systems Engineering, University of the Ryukyus, Okinawa 903-0213, Japan

Surface growth of Ni thin films electrodeposited on Ni(100) substrates has been investigated using atomic force microscopy. In the early stage of growth, islands nucleated on the Ni(100) substrates, which appear to be rectangular in cross section, grow laterally in the same crystallographic orientation. Growth surfaces display a normal scaling behavior characterized by the linear surface diffusion universality class. Along the time evolution, instability in growth occurs and a transition from two- to three-dimensional growth is observed. In this stage, surface growth obeys anomalous scaling characterized by a local roughness exponent $\zeta_{loc} = 1.0$, global scaling exponent $\zeta = 2.1$, and dynamic exponent $z = 1.0$.
 [DOI: 10.1149/1.1539499]

Manuscript submitted April 15, 2002; revised manuscript received August 22, 2002. Available electronically January 23, 2003.

Kinetic surface roughening has been a study of great interest for the past decade due to a good example of statistical scale invariance.[1] Studies on growing surfaces have revealed the presence of scaling exponents that determine universality classes. An interface width[2] $W(L,t)$ is usually related to the scaling exponents, which is defined as the root-mean-square (rms) of the fluctuations of the surface height $h(r,t)$

$$W(L,t) = \langle [h(r,t) - \bar{h}]^2 \rangle^{1/2} \quad [1]$$

where $\langle \ldots \rangle$ indicates an average over a system size L and $\bar{h}$ indicates an average of $h(r,t)$. The interface width has been recognized to obey the Family-Vicsek function[3]

$$W(L,t) = t^{\alpha/z} f(L/t^{1/z}) \quad [2]$$

which behaves as

$$f(u) = \begin{cases} u^{\alpha} & \text{for } u \ll 1 \\ \text{const} & \text{for } u \gg 1 \end{cases} \quad [3]$$

where α is the roughness exponent that describes the spatial scaling behavior and z is the dynamic exponent. The growth exponent β is given by $\beta = \alpha/z$, which represents the time-dependent dynamics of the surface roughness. These exponents α, β, and z determine the universality class to which a system belongs. The exponent α is usually calculated from the height-height correlation function[2] defined by

$$G(r,t) = \langle [h(r,t) - h(0,t)]^2 \rangle \propto r^{2\alpha} \quad [4]$$

However, recently it has been found that surface roughening in some theoretical models[4-7] and thin-film surfaces in growth[8-10] deviate from the Family-Vicsek function. Therefore an anomalous scaling function related to a local interface width has been proposed to describe the anomalous scaling behavior. The local interface width[4] $w(l,t)$ is defined by

$$w(l,t) = \begin{cases} t^{\beta^* l^{\zeta_{loc}}} & \text{for } l^z \ll t \ll L^z \\ t^{l/z} & \text{for } t \ll l^z \end{cases} \quad [5]$$

where $\beta^* = (\zeta - \zeta_{loc})/z$ is an anomalous growth exponent and l is a window size. The local interface width $w(l,t)$ is calculated over a window size l less than the system size L. Equation 5 indicates the presence of a crossover time for the time regime for $0 \ll t \ll L^z$ and the same form as the Family-Vicsek function for the time regime $t \ll l^z$. In the case of anomalous scaling, the correlation length $\xi \sim t^{1/z}$ and $z = \alpha/\beta$ do not hold. Hence, the anomalous scaling system has two roughness exponents: the local roughness ζ_{loc} independent of experimental conditions, and global roughness exponent ζ dependent on experimental conditions. In this paper, the anomalous scaling behavior in electrodeposition on single-crystal Ni substrates is presented.

Epitaxial growth in electrodeposition has been attempted for metal/metal systems.[11-13] Coadsorbates that usually exist in electrochemical environments affect growth modes classified as Frank-van der Merve growth or layer-by-layer growth (two-dimensional growth), Stranski-Krastanov growth (a transition from two- to three-dimensional growth), and Volmer-Weber growth (three-dimensional growth). Some kinds of coadsorbates are known to promote two-dimensional growth.[14,15] However, electrochemical processes have not yet produced epitaxial films thick enough for technological use. Theoretical models predict a critical two-dimensional island size[16] beyond which three-dimensional growth occurs. The transition is thought to correspond to a significant increase in the surface roughness, which is observed as a change from smooth surfaces to rough surfaces. In this study, the surface images measured by atom force microscopy (AFM) indicate the presence of the transition.

The data presented here indicate: (*i*) in the early stage of growth, the surface roughness exhibits the normal scaling behavior of the linear surface diffusion model, and (*ii*) as time proceeds, a transition from two- to three-dimensional growth is observed, which is characterized by anomalous scaling.

Experimental

Single-crystal Ni disks of 12 mm diam and 1 mm thick were prepared for cathode electrodes, which have (100) crystallographic surfaces within an accuracy of 2°. The single-crystal Ni disks were polished using three kinds of pastes including diamond powders of 5, 1, and 0.1 μm diam, and finally lapped with a solution of 0.05 μm colloidal silica in diameter. The surfaces appear to be mirror-like and have the rms roughness of 1.2 nm for a widow size of 2 μm. Then the single-crystal Ni disks were electrochemically etched in a H_2SO_4-$C_3H_5(OH)_3$ (glycerin)-H_2O solution. As pointed out in Ref. 11, nickel oxides will be left on the etched surfaces. In our preliminary experiments, as surface growth on (100) surfaces that were polished mechanically did not display two-dimensional growth, (100) surfaces etched electrochemically after mechanical polishing were chosen for this study. Figure 1 shows AFM images of the single-crystal Ni disk before and after electrochemical etching. The vertical scale is magnified by a factor of 18 in order to enhance viewing. It can be seen from Fig. 1b that the etched Ni surface has no flaws made mechanically during polishing. The single-crystal Ni disk and carbon plate for anode electrodes cleaned by a wet process were located parallel in a still bath containing (g/L): nickel sulfamate, 600; nickel chloride, 5; and boric acid, 40. The bath was maintained at pH 4 and a temperature of 323 K. A direct current was applied between the two electrodes. The direct current density in

* Electrochemical Society Active Member.
z E-mail: saitou@tec.u-ryukyu.ac.jp

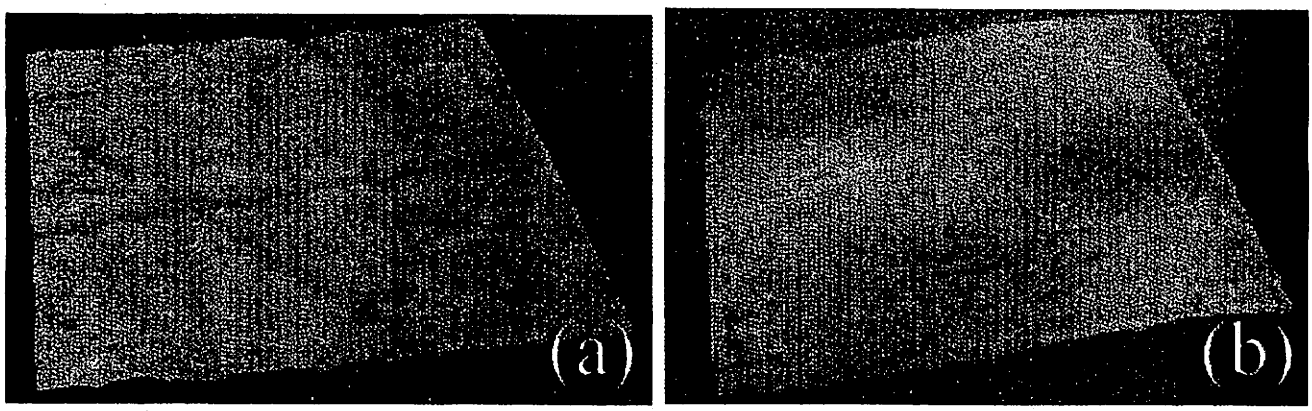

Figure 1. AFM images of the single-crystal Ni(100) surfaces: (a) mechanically polished and (b) electrochemically etched surface after mechanical polishing. The vertical scale of each image with a resolution of 512 × 512 pixels was magnified by a factor of 18 in order to enhance viewing.

electrodeposition was 0.1 mA/cm^2, at which the growth rate is about 0.2 ML (monolayers)/s. Only one current density is chosen in this study according to the scaling hypothesis in modern statistical mechanics,[17,18] which requires that the scaling exponents and the relationships between them are insensitive to specific systems and experimental conditions. Nickel thin films were electrodeposited on the indium tin oxide (ITO) glass of 1 × 1 cm^2. The system size L in this experiment is 1 cm. The nickel thin films were grown for the growth time ranging from 500 to 80,000 s. The nickel deposits were scanned in air with AFM that has a resolution of 512 × 512 pixels. The AFM images with different scan regions of 1000 × 1000, 2000 × 2000, and 5000 × 5000 nm^2 were used for the calculations of the scaling exponents.

Determination of Local Exponents ζ_{local}

In this study, the local roughness exponent ζ_{loc} is determined by two methods: the Hurst rescaled range (R/S) analysis[19] and the Fourier transformation method.[20] The formula for the calculation of the exponent ζ_{loc} in the R/S analysis is as follows: An arbitrary radius on the AFM images is represented by r_k

$$R(k,t)/S(k,t) \propto r_k^{\zeta_{loc}} \quad [6]$$

where

$$R(k,t) = \max_{0\le i\le k}[X(i,t)] - \min_{0\le i\le k}[X(i,t)]$$

$$S(k,t) = \left[k^{-1}\sum_{i=1}^{k}(h(r_i,t) - \langle h(r,t)\rangle_i)^2\right]^{1/2} \quad [7]$$

$$X(k,t) = \sum_{i=1}^{k}[h(r_i,t) - \langle h(r,t)\rangle_k]$$

First we calculate $X(k,t)$ within a radius r_k on the AFM image. Next, we find the maximum and minimum change of $X(k,t)$ and normalize $R(k,t)$ by the standard deviation $S(k,t)$.

The Fourier transformation method is to determine the local roughness exponent ζ_{loc} from the power spectrum. The power spectrum of $H(f,t)$ that is the Fourier transform of $h(r,t)$ is given by

$$|H(f,t)|^2 \propto f^{-\gamma} \quad [8]$$

where f is the frequency and γ is a constant value. The local roughness exponent is expressed by the slope γ

$$\zeta_{loc} = (\gamma - 2)/2 \quad [9]$$

Results and Discussion

Discussion of AFM images.—Figure 2 shows typical AFM images of nickel electrodeposits grown for different times. In the early stage of growth, many islands which appear to be rectangular in cross section grow laterally with time and coalesce into large sizes (Fig. 2a-c). In addition, the islands grow not in the random crystallographic direction but uniformly in the same one. The surface morphology remains surprisingly flat and appears to evolve obeying the two-dimensional growth mode. A line scan of Fig. 2b appears in Fig. 3a and clearly shows the existence of flat surfaces of the islands. The height h in Fig. 3a corresponds to 10 ML. But in the later growth time regime, the lateral growth rate of the islands decreases and the surfaces become rough (Fig. 2d-f). A line scan of Fig. 2e is shown in Fig. 3b that indicates that the heights of the islands increase rapidly. Figure 4 shows a plot of the average diameter of the islands *vs.* time. It can be seen that the diameter appears to saturate with time.

Scaling analysis.—For a finite window size l, the local width is expected to scale as $w(l,t) \sim t^{\beta}$. Figure 5 shows plots of $w(l,t)$ *vs.* l in a log · log scale for l = 1000 and 5000 nm. In our experiment, along the time evolution, we find that the exponent β takes up to three different values. At the early time, we measure β = 0.25 ± 0.07, which is close to that of the linear surface diffusion model for MBE[21,22] described by

$$\partial h(r,t)/\partial t = -K\nabla^4 h(r,t) + \eta \quad [10]$$

where η denotes the random fluctuation in deposition and K is a constant. The mean roughness exponent, α = 0.96 ± 0.05 is determined as shown in Fig. 6. In this time regime, the surface morphology remains flat and obeys the two-dimensional growth mode.

In the further time regimes, instability in growth takes place, which corresponds to a greater increase in the slopes of islands and is associated with a transition from two-dimensional to three-dimensional growth. This instability is reflected in the very large values of β = 2.1 ± 0.1 and 1.1 ± 0.2, which belong to no universality classes for normal scaling and indicate anomalous values by far greater than 1/2. In addition, this may correspond to the presence of a critical island diameter[16] for the transition from two- to three-dimensional growth. Islands comprise many atomic layers and a layer nucleates on the top of the island at the critical island diameter. Owing to the diameter of the islands beyond the critical size that is an order of $(4a^2D/F)^{1/6}$ where a is the lattice constant, D is the surface diffusion coefficient of adatoms, and F is the incident atom flux, this transition, *i.e.*, an abrupt increase in the local interface width takes place as shown in Fig. 5. Hence we can divide the experimental time into two time regimes: the early stage of growth

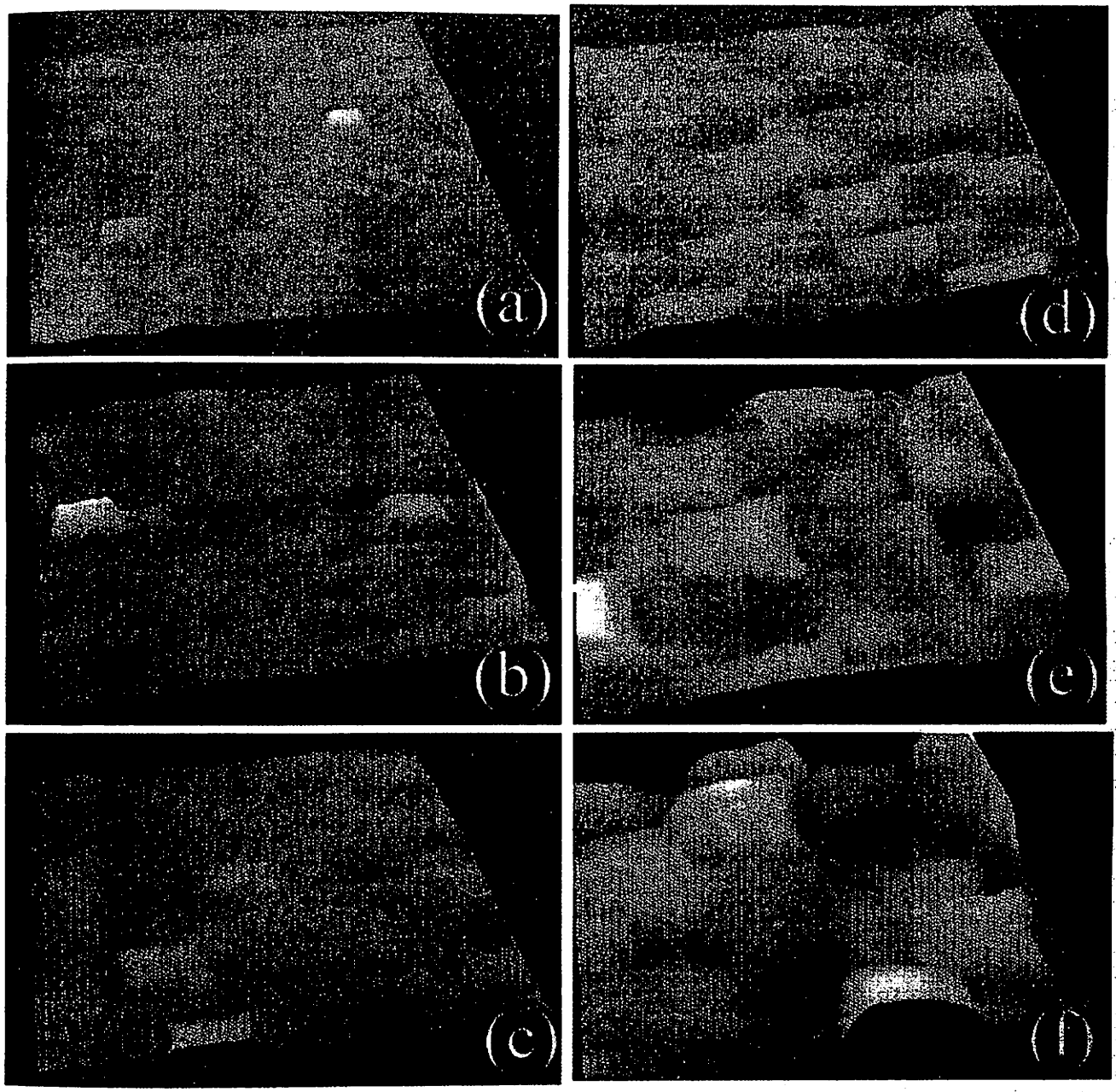

Figure 2. AFM images of Ni thin-film surfaces grown on the Ni(100) substrates for different growth times: (a) 4500, (b) 6000, (c) 8000, (d) 16,000, (e) 32,000, and (f) 60,000 s. The vertical scales of (a-d) and (e,f) images were magnified by a factor of 18 and 5, respectively, in order to enhance viewing.

in which surface growth obeys normal scaling characterized by the linear growth model universality class, and the later stage of growth in which the surface morphology is expected to obey the anomalous scaling function in Eq. 5.

In the later time regime, the local roughness exponent ζ_{loc} is determined by the Hurst rescaled range (R/S) analysis and the Fourier transformation method. Figure 7a and b shows typical log-log plots of $R(k,t)/S(k,t)$ *vs.* r_k and $|H(f,t)|^2$ *vs.* the frequency f. The AFM image of 2000 × 2000 nm^2 electrodeposited for 25,000 s was used for the calculations in Fig. 7. The slope of the best straight-fitted line to the data in Fig. 7a gives the local roughness exponent $\zeta_{loc} = 1.0$. The average ζ_{loc} for the nickel films grown for 10,000-80,000 s becomes 0.99 ± 0.05. In Fig. 7b, the slope of γ best fitted to the data yields 3.92, which gives a value of $\zeta_{loc} = 0.96$. In a similar fashion, the average value of ζ_{loc} for the nickel films grown for 10,000-80,000 s using the Fourier transform method becomes 1.0 ± 0.08, which is independent of the window length l. Now, it is concluded that the local roughness ζ_{loc} obtained from the two methods is 1.0. In the case of normal scaling, the roughness exponent α is equal to the local roughness ζ_{loc}. In this study the roughness exponent α for 500-10,000 s becomes 0.96 ± 0.05. The values of the slopes in Fig. 5 and 7 yield the global roughness exponent ζ of 2.1 and the dynamical exponent z of 1.0. Thus we can determine the

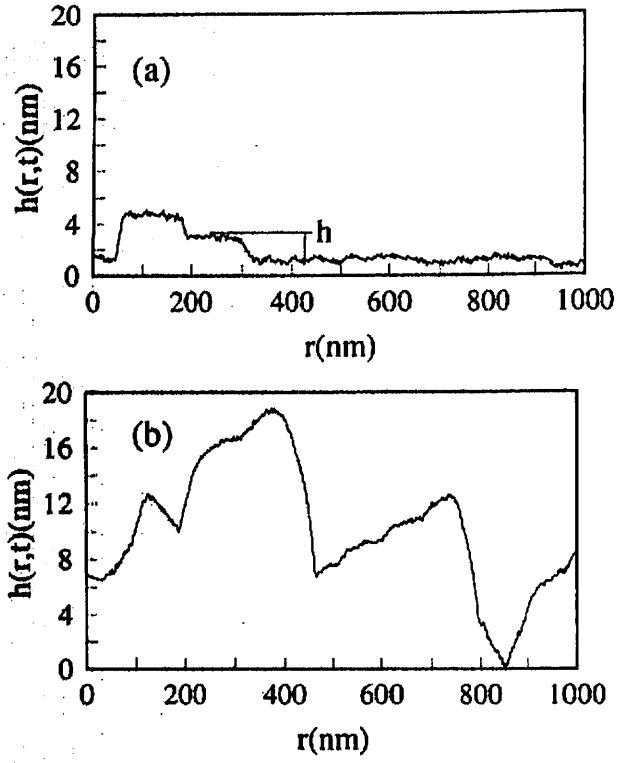

Figure 3. One-dimensional line scans from AFM images of Fig. 2b and e; t = (a) 6000 and (b) 32,000 s.

universality class of the anomalous scaling characterized by $\zeta_{loc} = 1.0$, $\zeta = 2.1$, and $z = 1.0$

Conclusions

Ni thin films were grown by electrodeposition on Ni(100) substrates at a very low current density. In the early stage of growth, islands nucleated on the Ni(100) surface, which appears to be rectangular in cross section, grows laterally in the same crystallographic orientation, and displays normal scaling that belongs to the linear diffusion growth universality class. Along the time evolution, instability in growth takes place and a transition from two to three-

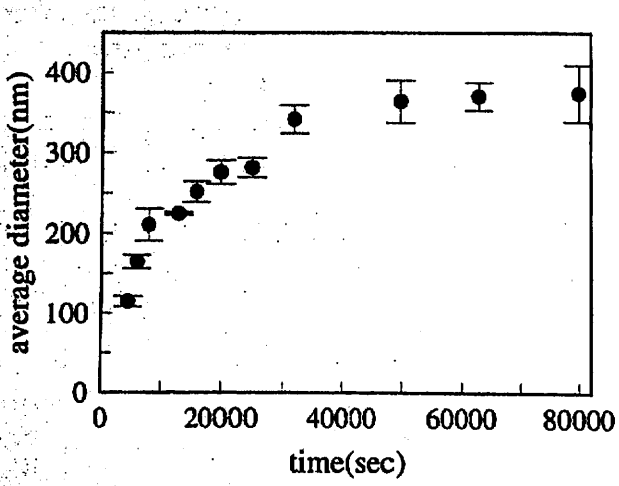

Figure 4. Time evolution of the average diameter of islands.

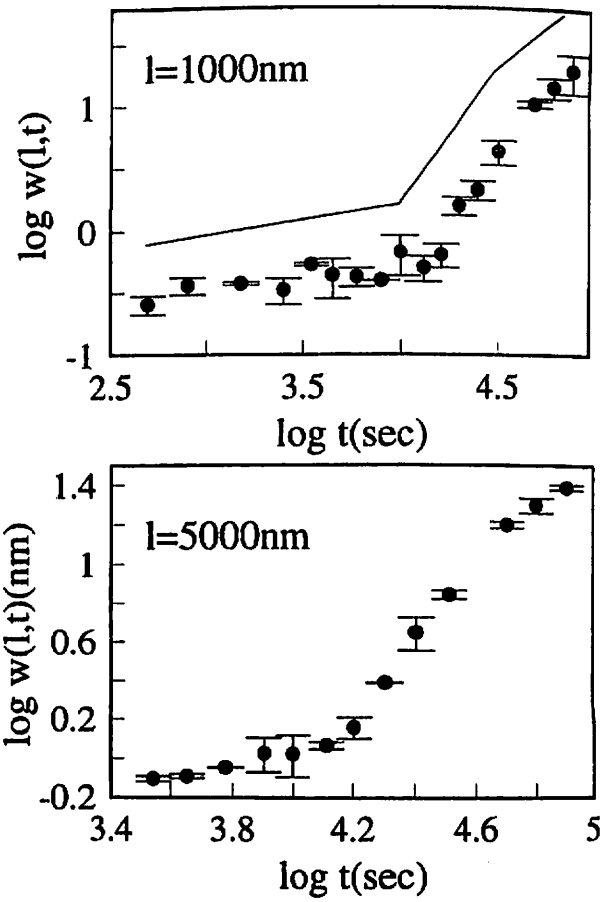

Figure 5. Log-log plots of local width $w(l,t)$ *vs.* time t for the different window sizes: (a) l = 1000 and (b) 5000 nm. The slopes take up to three different values. The straight lines are plotted as a guide for the eye.

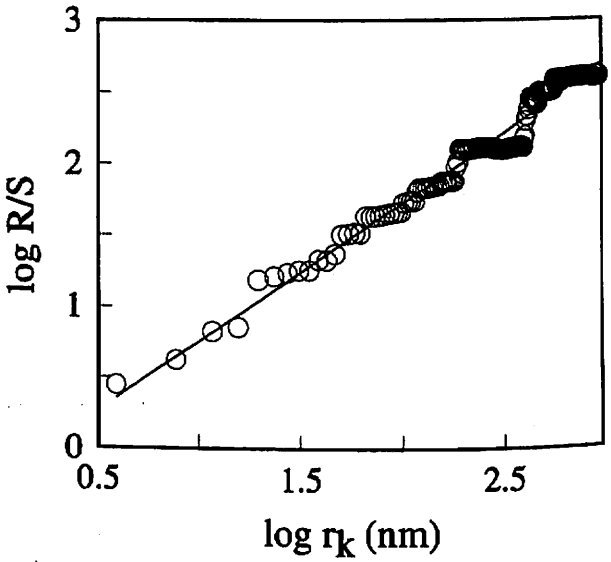

Figure 6. Hurst plot for the AFM image of 2000 × 2000 nm^2 electrodeposited for 3500 s. The solid straight line best fitted to the data indicates a slope of 0.97.

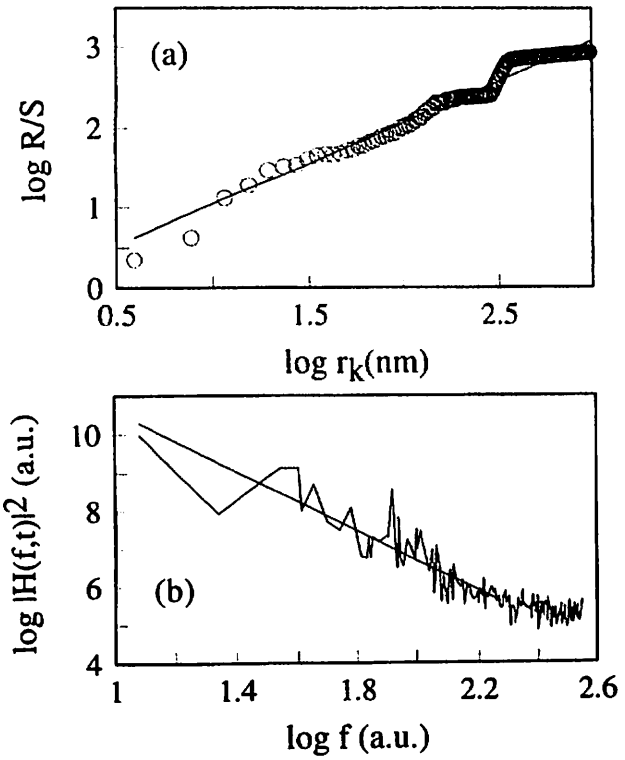

Figure 7. Determining the local roughness ζ_{loc} by two methods: (a) R/S analysis and (b) the Fourier transform method. The AFM image of 2000 × 2000 nm^2 electrodeposited for 25,000 s was used for the calculations.

dimensional growth is observed. In this stage, surface growth exhibits an anomalous scaling behavior characterized by the local roughness exponent $\zeta_{loc} = 1.0$, global scaling exponent $\zeta = 2.1$, and dynamic exponent $z = 1.0$.

Acknowledgments

This work was supported by Grant-in-Aid for Scientific Research (C), no. 13650029, by the Ministry of Education, Science, and Culture of Japan.

The University of the Ryukyus assisted in meeting the publication costs of this article.

References

1. A. C. Levi and M. Kotrla, *J. Phys. C*, 9, 299 (1997).
2. A.-L. Barabási and H. E. Stanley, *Fractal Concepts in Surface Growth*, Cambridge University Press, New York (1995).
3. F. Family and T. Vicsek, *Dynamics of Fractal Surfaces*, World Scientific, Singapore (1991).
4. J. M. López, M. A. Rodríguez, and R. Cuerno, *Phys. Rev. E*, **56**, 3993 (1997).
5. M. Castro, R. Cuerno, A. Sánchez, and F. D-Adame, *Phys. Rev. E*, **57**, R2491 (1998).
6. J. M. Ramasco, J. M. López, and M. A. Rodríguez, *Phys. Rev. Lett.*, **84**, 2199 (2000).
7. N. Pand and W. Tzeng, *Phys. Rev. E*, **61**, 3559 (2000).
8. N.-H. Yang, G. C. Wang, and T.-M. Lu, *Phys. Rev. Lett.*, **73**, 2348 (1994).
9. J. H. Jeffries, J. K. Zuo, and M. M. Craig, *Phys. Rev. Lett.*, **76**, 4931 (1996).
10. S. Huo and W. Schwarzacher, *Phys. Rev. Lett.*, **86**, 256 (2001).
11. F. A. Möller, J. Kintrup, A. Lachenwitzer, O. M. Magnussen, and R. J. Behm, *Phys. Rev. B*, **56**, 12506 (1997).
12. J. C. Ziegler, A. Reitzle, O. Bunk, J. Zegenhagen, and D. M. Kolb, *Electrochim. Acta*, **45**, 4599 (2000).
13. F. Maroun, S. Morin, A. Lachenwitzer, O. M. Magnussen, and R. J. Behm, *Surf. Sci.*, **460**, 249 (2000).
14. J. P. Hoare, *J. Electrochem. Soc.*, **133**, 2491 (1986).
15. K. Sieradzki, S. R. Brankovic, and N. Dimitrov, *Science*, **284**, 138 (1999).
16. J. Tersoff, A. W. D. van der Gon, and R. M. Tromp, *Phys. Rev. Lett.*, **72**, 266 (1994).
17. N. Goldenfeld, *Lecture on Phase Transitions and the Renormalization Group*, Perseus Books Publishing, Cambridge, MA (1992).
18. J. J. Binney, N. J. Dowrick, A. J. Fisher, and M. E. J. Newman, *The Theory of Critical Phenomena*, Oxford University Press, New York (1995).
19. J. Feder, *Fractals*, Plenum, New York (1988).
20. A. I. Oliva, E. Anguiano, J. L. Sacedón, and M. Aguilar, *Phys. Rev. B*, **60**, 2720 (1999).
21. D. E. Wolf and J. Villain, *Europhys. Lett.*, **13**, 389 (1990).
22. S. Das Sarma and P. Tamborenea, *Phys. Rev. Lett.*, **66**, 325 (1991).